Supporting Information

Hydrophobic Organic Spacer Cation for Improving Moisture Resistance and Efficiency in Mixed-Dimensional Perovskite Solar Cells

Prasun Kumar,[a, b] Satinder Kumar Sharma,[c] Ranbir Singh*[, a, b]

[a]School of mechanical and Materials Engineering (SMME), Indian Institute of Technology (IIT) Mandi, Mandi, Himachal Pradesh, 175005, India

[b]Advanced Energy Conversion Laboratory (AECL), Indian Institute of Technology (IIT) Mandi, Mandi, Himachal Pradesh, 175005, India

[c]School of Computing and Electrical Engineering (SCEE), Indian Institute of Technology (IIT) Mandi, Mandi, Himachal Pradesh, 175005, India

Corresponding author email ID ranbir@iitmandi.ac.in

Experimental Section:

(a) Materials: Methyl ammonium iodide (MAI, 99.9%), formamidinium iodide (FAI), lead (II) iodide (PbI_2, 99.99%), and were purchased from TCI Pvt. Ltd. Dimethylformamide (DMF), dimethyl sulfoxide (DMSO), tin (IV) oxide (SnO_2), anhydrous ethanol, chlorobenzene, acetonitrile, isopropyl alcohol, trimethylsulfoxonium chloride (TMSCl, 98%), bis(trifluoro-methane)-sulfonamide lithium salt (Li-TFSI), ethanol, 4-tert-butylpyridine (TBP), tris(2-(1H-pyrazol-1-yl)-4-tert-butylpyridine) cobalt(III) tris(bis(trifluoromethyl sulfonyl) imide) (FK209), toluene, and 2,20,7,70-tetrakis-(N,N-di-p-methoxyphenylamine)-9,90-spirobifluorene (Spiro-OMeTAD) were purchased from Sigma–Aldrich. All materials were utilized without additional purification.

(b) Device fabrication: Our fabricated device with glass/indium-doped tin oxide (ITO)/ SnO_2/$MAFA(TMS)_XPbI_{3-X}Cl_X$/spiro-OMeTAD/gold (Au) structured were fabricated within a glove box. Initially, etched ITO substrates were cleansed utilizing detergent, deionized water, acetone, and isopropyl alcohol. The substrates were then placed in an ozone plasma treatment for 30 min. After that, 15% tin (IV) oxide colloidal dispersion in H_2O was deposited on the

ITO glass by spin coating (2500 rpm for 25sec) and then heated for 30 min at 140°C. For $MAFAPbI_3$ (PVK) thin film deposition, MAI:FAI:PbI_2 (1.40 M:0.10 M:1.40 M) were mixed in 1mL solvent (8:2 anhydrous DMF:DMSO). Then, the precursor was spin-coated onto the SnO_2 layer with an antisolvent method at spin rate of 1000 rpm for 10s and 4000 rpm for 30 sec. After 10s of spinning at 4000 rpm, 280 µL of CB was immediately dripped on the film followed by thermal annealing at 120°C for 30min. Here, CB was employed as an antisolvent for the fast crystallization of the perovskites. Additionally, we dissolved TMSCl:PbI_2 (0.5M:0.5M) in 1 mL solvent (7:3 anhydrous DMF:DMSO) and doped this solution with different concentrations (0.5, 1, 2, 4, and 8 mg) in PVK solution. Then, the precursor was spin-coated onto the SnO_2 layer with an antisolvent method as similar as PVK deposition. To deposit HTL on perovskite layer via spin coating (spin rate of 3000rpm, time 20s), we used spiro-OMeTAD solution containing 73mg spiro-OMeTAD per 1mL chlorobenzene with Li-TFSI (28 µL; mother solution: acetonitrile, 530 mg /mL), TBP (28 µL), and FK209 (18µL; mother solution: acetonitrile, 300mgmL 1). Finally, ~90 nm thick Au was thermally evaporated as a top electrode under vacuum ($<5\times10^{-6}$ Torr) using a metal mask.

(c) ***Photophysical and Morphological Characterization:*** UV-visible absorption and steady-state PL spectra were measured using UV2080N (Analytical Technologies Ltd.) and Agilent Cary Eclipse Fluorescence spectrophotometer, respectively. The samples were excited at 520 nm for PL measurements. FTIR spectrometer were measured by PerkinElmer, UATR Two. Raman spectra and TRPL were measured by RENISHAW inVia Raman Microscope and DeltaFlex (HORIBA Scientific) respectively. Scanning electron microscopy images were taken by a FEI Nova Nano SEM-450 instrument. An AFM system (Dimension Icon from Bruker) was employed to measure the roughness of perovskite films. XRD patterns of different films were obtained by Rigaku Smart Lab 9kW rotating anode diffractometer using Cu Kα (λ=1.5405Å)

radiation as a source. EDS measurements were performed by a EDAX by AMETEK. The contact angle measurements were carried out using a Surface Electro-Optics (SEO) Phoenix instrument.

(d) ***Electrical Characterizations:*** Current density-voltage (J-V) characteristics of the devices were recorded by a Keithley 2400 source meter under one-sun irradiation (100 mWcm^2) from a solar simulator (TriSOL). The intensity of the simulator was calibrated using a mono-Si solar cell (SN-1000-TC-K-QZ, VLSI standards S/N 105100602) certified by VLSI Standards. For indoor measurement. the indoor LED light simulator consists of commercial purchase Osram E27 LED lamps, which are calibrated for 1000 lx (321.6 µW/cm^2) with standard luxmeter and optical power meter (PM160) from Thorlabs. The scan rate during J-V characteristics measurements was fixed at 0.05V/s. The contact angle of a water droplet was estimated from images captured using a DSA100 analyzer. EIS measurements were conducted in the Auto lab (MAC90173, Metrohm 302N) electrochemical workstation.

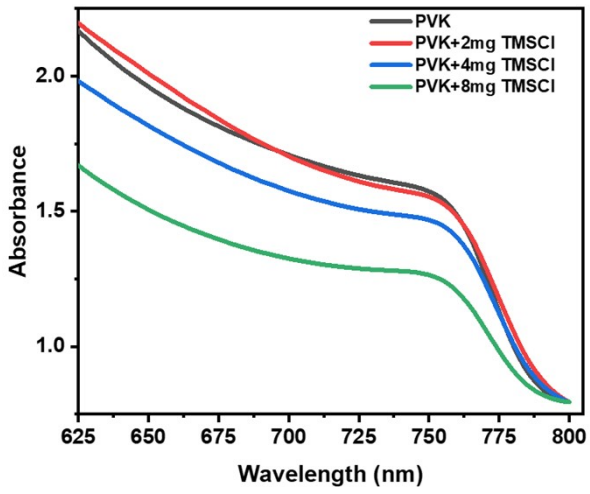

Figure S1. Graph of UV-Vis spectra for higher concentrations of TMSCl doping.

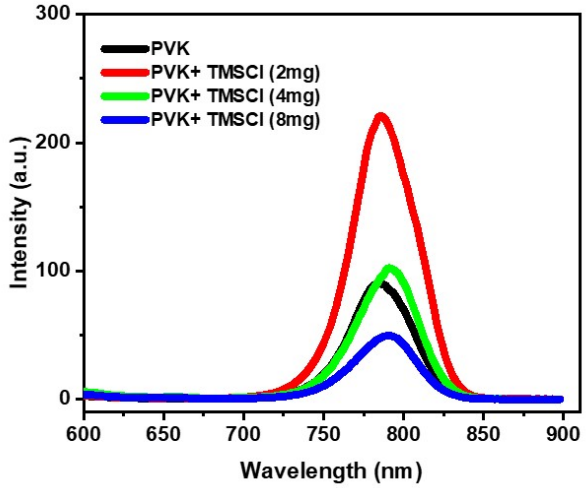

Figure S2. Graph of steady state PL for higher concentrations of TMSCl doping.

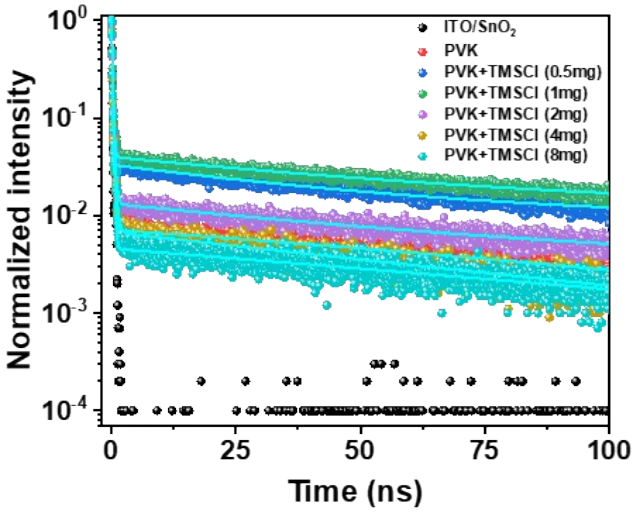

Figure S3. TRPL graphs of doping of different concentrations of TMSCl in PVK.

Table S1. Illustration of the fitting results of different doped films with a bi-exponential decay function.

Device structure	τ_1 (ns)	A (%)	τ_2 (ns)	B (%)	τ_{avg} (ns)
PVK (ref.)	0.177	98	64.48	2	1.46
PVK+TMSCl (0.5mg)	0.44	94	73.5	6	4.82
PVK+TMSCl (1mg)	0.46	95	103.50	5	5.58
PVK+TMSCl (2mg)	0.173	98	111.01	2	2.32
PVK+TMSCl (4mg)	0.323	98	54.96	2	1.41
PVK+TMSCl (8mg)	0.119	97	41.08	3	1.33

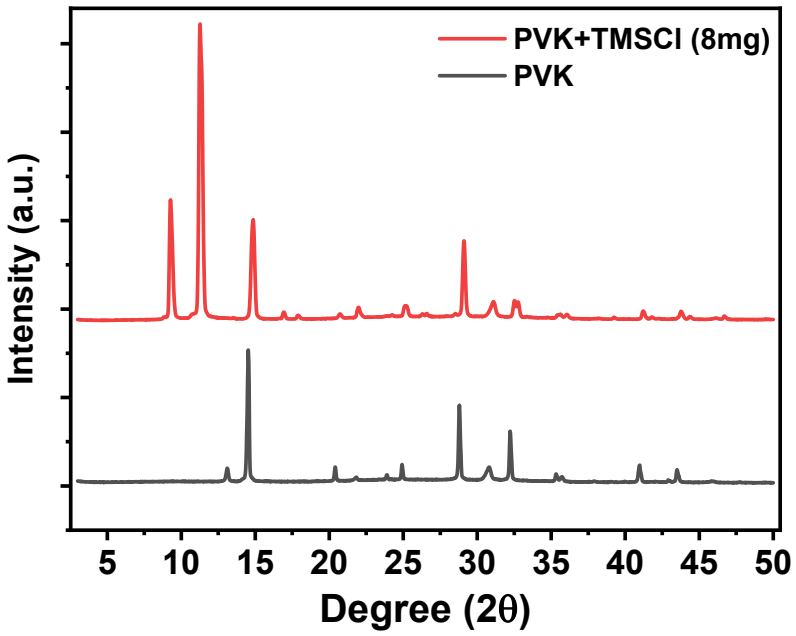

Figure S4. XRD graph for higher concentration of TMSCl doping.

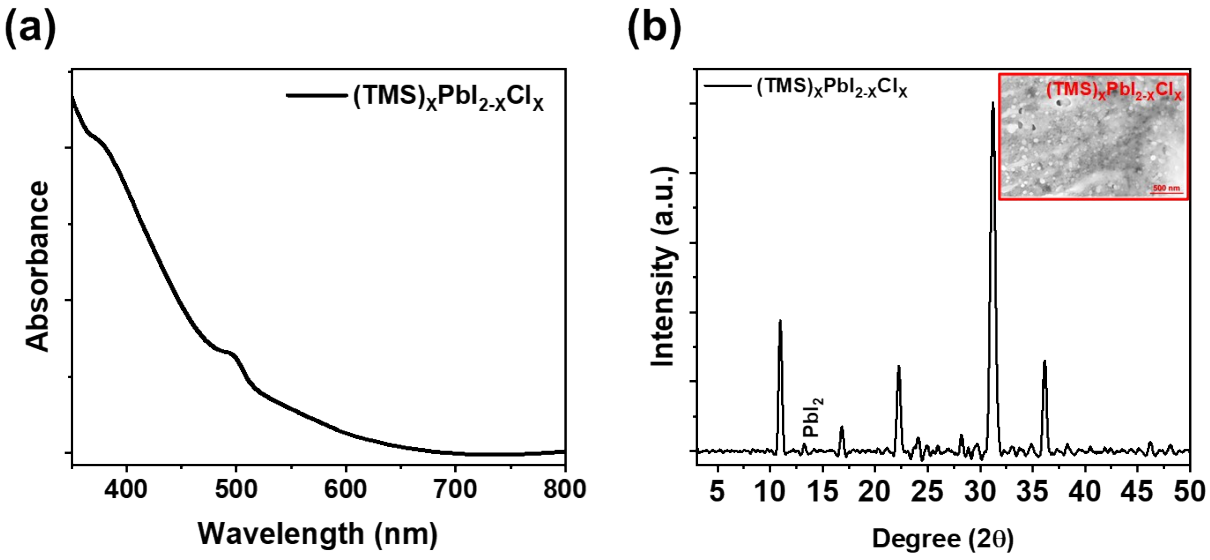

Figure S5. (a) Absorption spectra of $(TMS)_XPbI_{2-X}Cl_X$ film, (b) XRD graph for of $(TMS)_XPbI_{2-X}Cl_X$ film with SEM image.

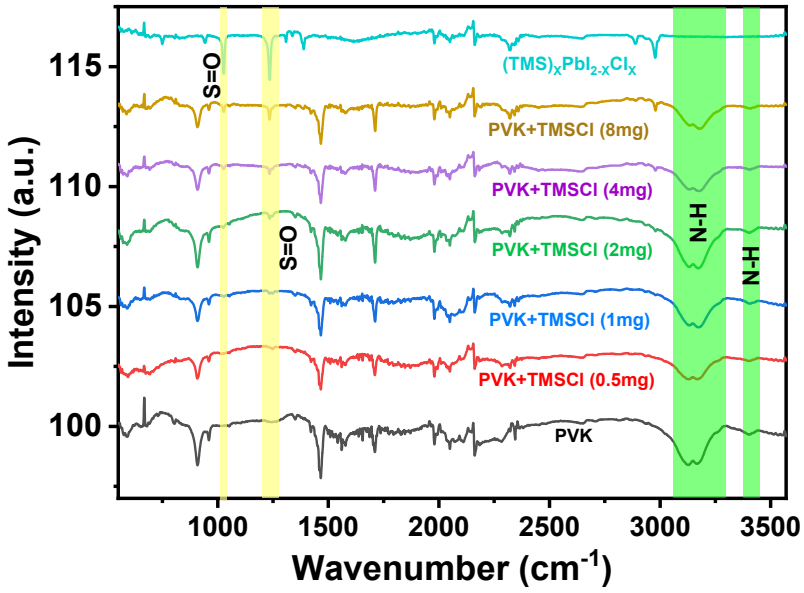

Figure S6. The FTIR spectra for PVK, different concentrations of TMSCl doping in PVK and $(TMS)_XPbI_{2-X}Cl_X$.

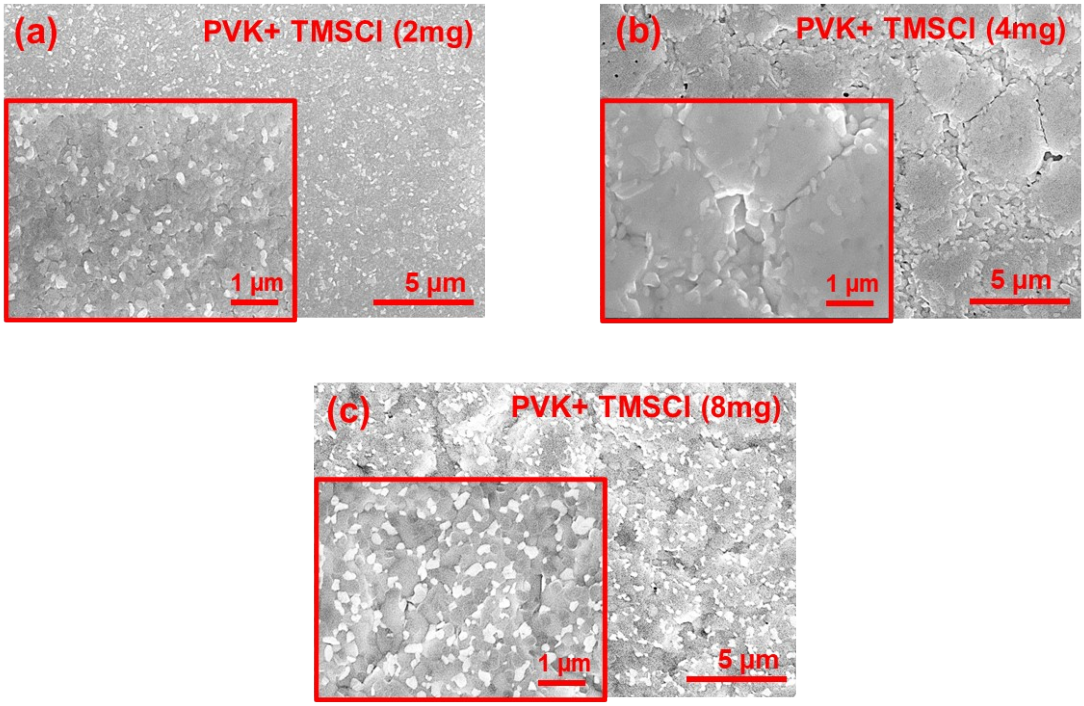

Figure S7. SEM images for higher concentration of TMSCl doping.

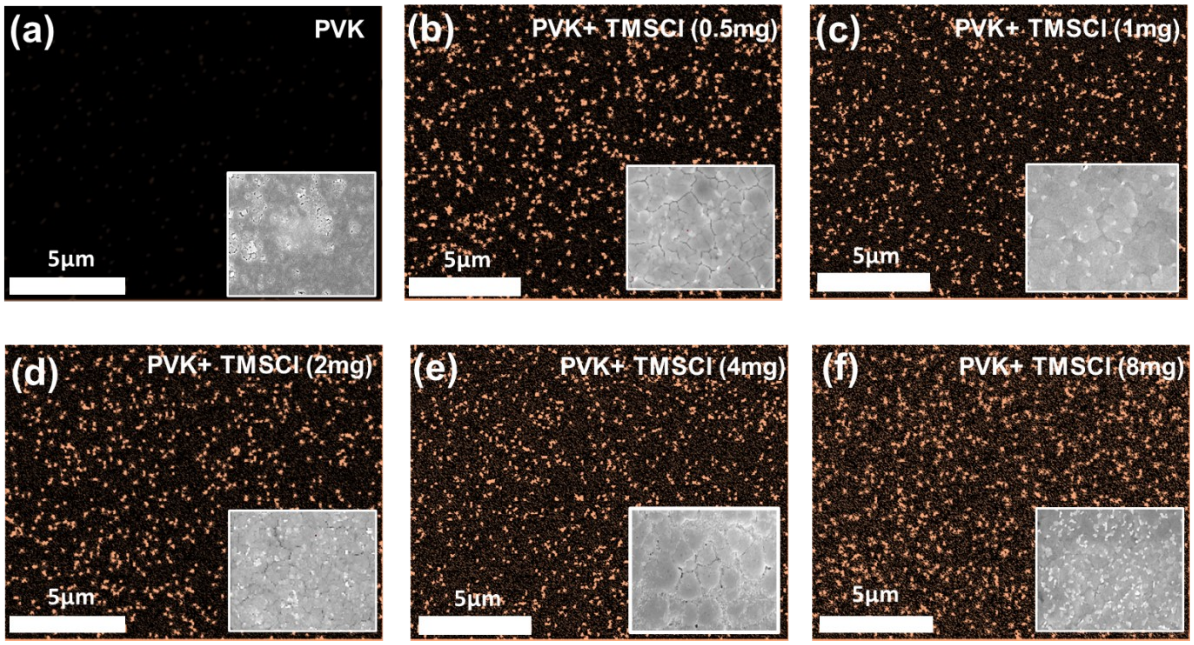

Figure S8. EDS mapping images of PVK and different concentration of TMSCl additive with live SEM images all through mapping.

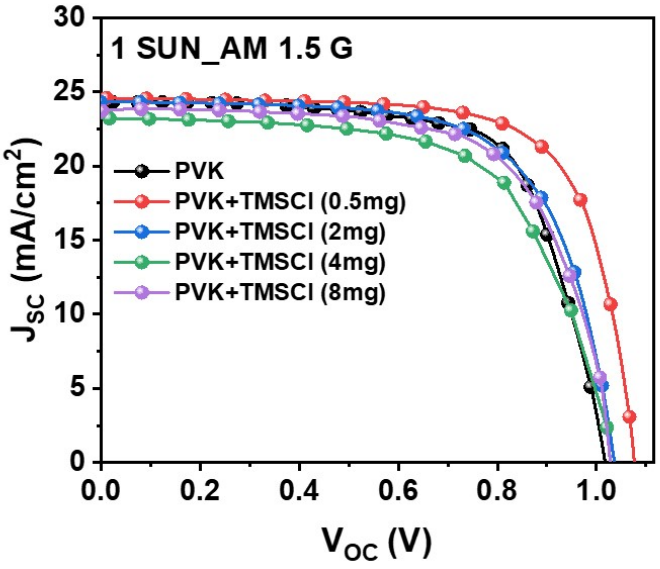

Figure S9. J-V characteristics for higher concentration of TMSCl doping under one sun condition.

Table S2. Illustration of device parameters for different doping concentration of TMSCl doping under one sun condition.

Device structure	V_{OC} (V)	J_{SC} (mA/cm^2)	FF (%)	PCE (%)
PVK (ref.)	1.02	24.46	71.26	17.82
PVK + TMSCl (0.5mg)	1.06	24.58	73.80	19.22
PVK + TMSCl (2mg)	1.03	24.32	70.89	17.75
PVK + TMSCl (4mg)	1.03	23.32	65.97	15.84
PVK + TMSCl (8mg)	1.03	23.69	67.86	16.55

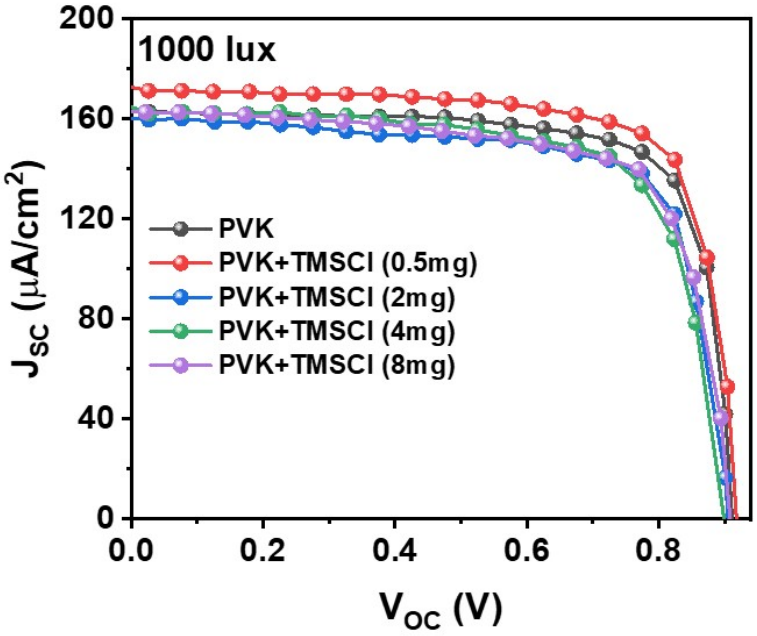

Figure S10. J-V characteristics for higher concentration of TMSCl doping under indoor lighting condition.

Table S3. Illustration of device parameters for different doping concentration of TMSCl doping under indoor lighting condition.

Device structure	V_{OC} (V)	J_{SC} (mA/cm^2)	FF (%)	PCE (%)
PVK (ref.)	0.91	162.98	73.90	29.85
PVK + TMSCl (0.5mg)	0.91	176.03	73.29	31.59
PVK + TMSCl (2mg)	0.90	162.79	72.16	28.30
PVK + TMSCl (4mg)	0.89	160.82	69.84	28.16
PVK + TMSCl (8mg)	0.90	162.72	71.75	28.65

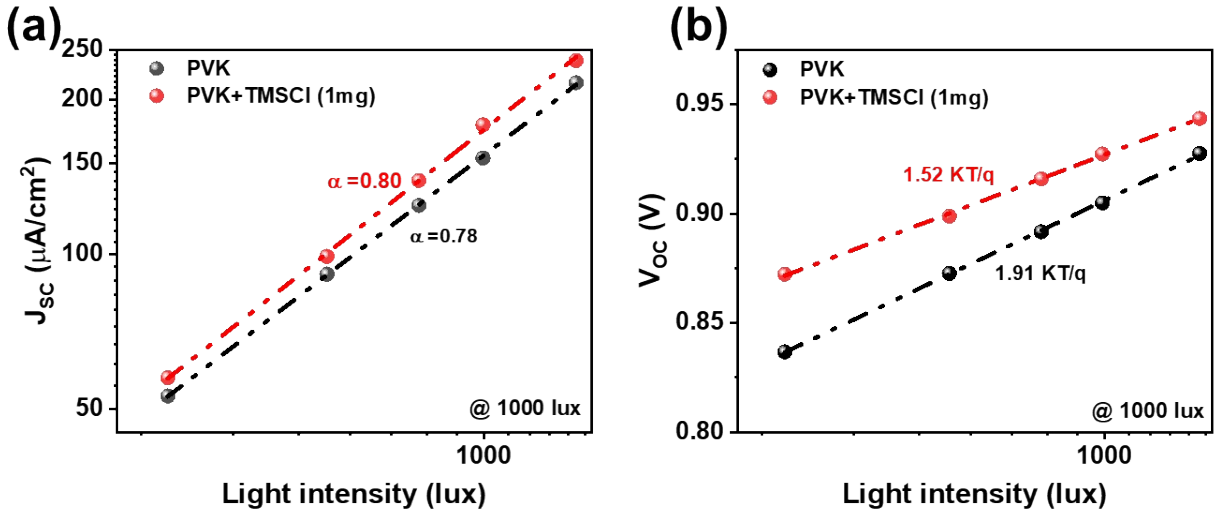

Figure S11. (a) J_{SC} verses light intensity plot and (b) V_{OC} verses light intensity plot under indoor lightening conditions.

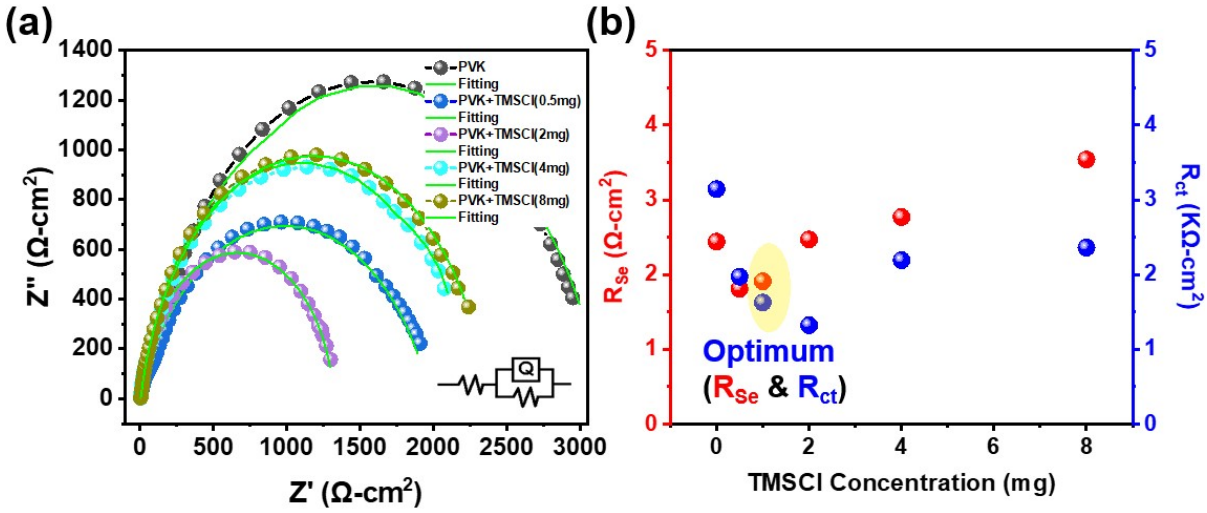

Figure S12. (a) EIS graphs for different concentration of TMSCl doping under dark condition and (b) optimized TMSCl concentration in EIS.

Table S4. Illustration of impedance parameters for different doping concentration of TMSCl doping under dark condition.

Device structure	R_{se} (Ω-cm2)	R_{ct} (Ω-cm^2)
PVK (ref.)	2.24	3144
PVK + TMSCl (0.5mg)	1.81	1972
PVK +TMSCl (1mg)	1.91	1625

PVK +TMSCl (2mg)	2.47	1320
PVK + TMSCl (4mg)	2.77	2193
PVK + TMSCl (8mg)	3.54	2361

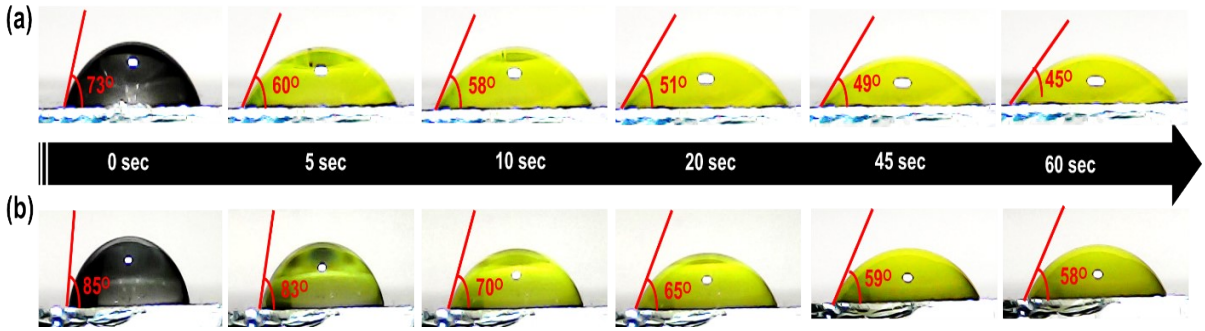

Figure S13. Images of contact angle measurement with time variation for (a) PVK and (b) PVK+TMSCl(1mg).

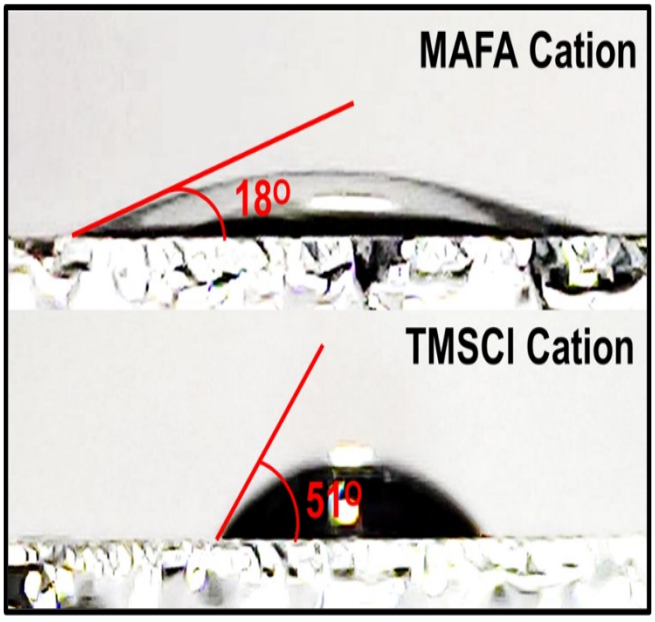

Figure S14. Image of contact angle measurement of MAFA and TMSCl cations.

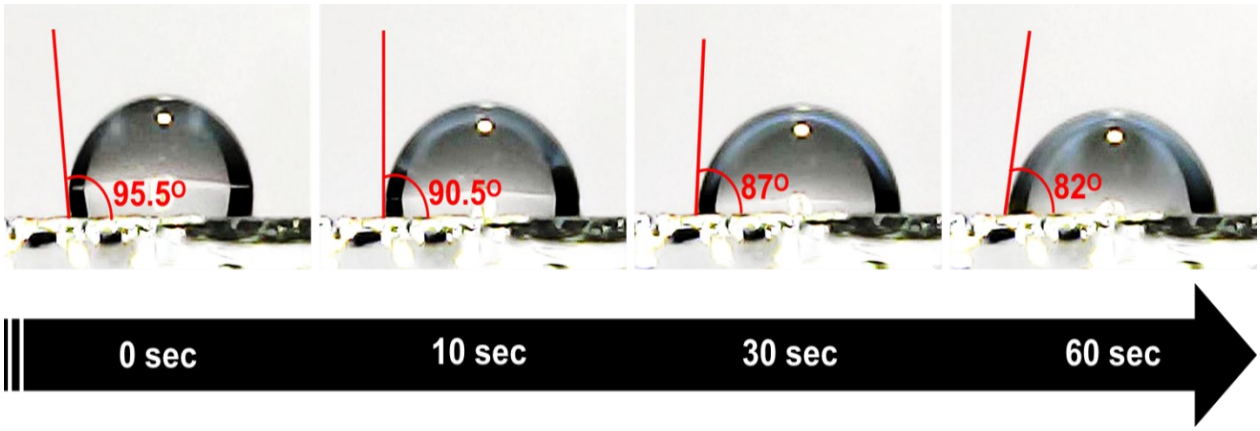

Figure S15. Images of dynamic contact angle measurement of $(TMS)_XPbI_{2-X}Cl_X$ film with time variation.

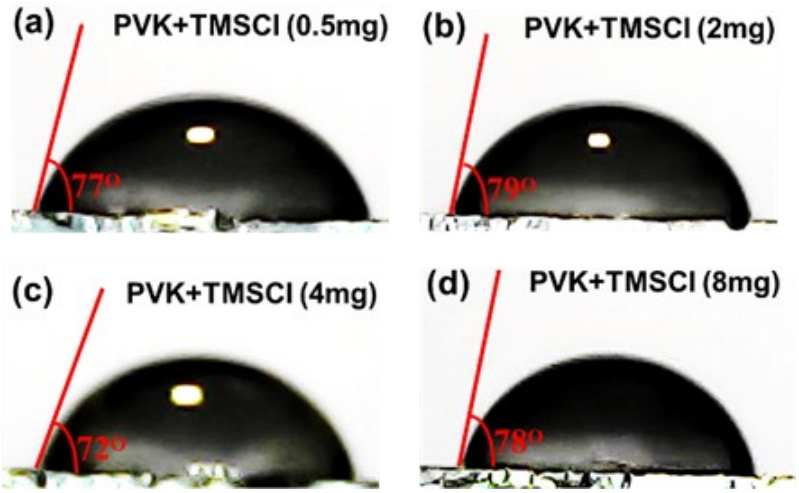

Figure S16. Contact angle measurements at different doping concentrations of TMSCl in PVK.

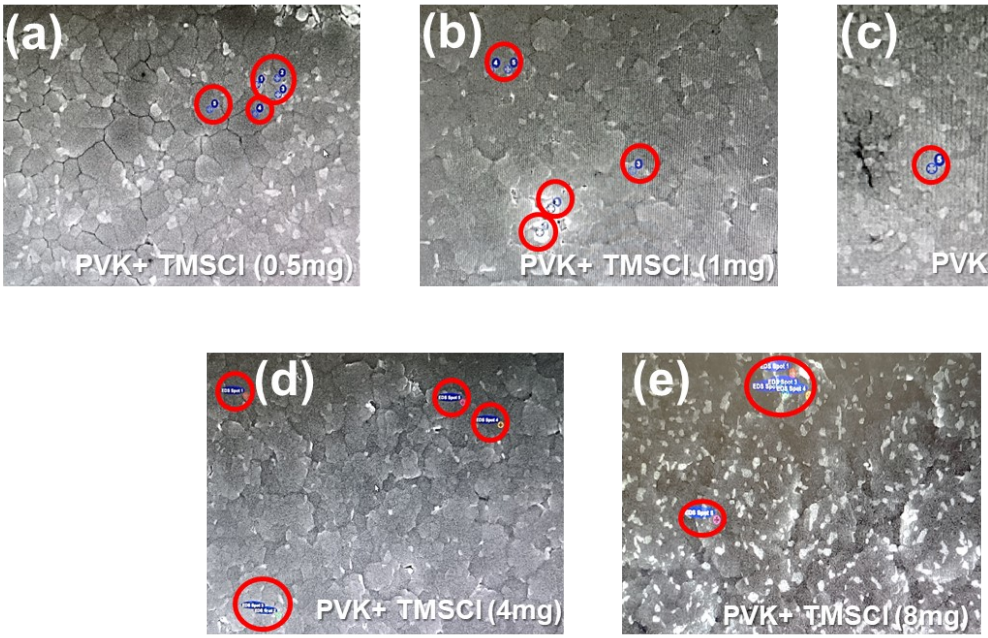

Figure S17. Images of EDS mapping of Cl weight percentage at grain boundaries and inside grains for different doping concentration of TMSCl cation